Chemical Engineering Science 158 (2017) 50–57

Contents lists available at ScienceDirect

Chemical Engineering Science

journal homepage: www.elsevier.com/locate/ces

The effect of operating conditions on the residence time distribution and axial dispersion coefficient of a cohesive powder in a rotary kiln

Ingrid J. Paredes[a], Bereket Yohannes[a], Heather Emady[a], Benjamin J. Glasser[a], William G. Borghard[a], Fernando Muzzio[a], Alberto M. Cuitiño[a,*], Jean Beeckman[b], Samia Ilias[b], Paul Podsiadlo[b], Eric Jezek[b], Joseph Baumgartner[b]

[a] Rutgers, the State University of New Jersey, Piscataway, NJ, United States
[b] ExxonMobil Research and Engineering Company, Annandale, NJ, United States

ARTICLE INFO

Keywords:
Rotary kilns
Calcination
Particle technology
Powder flow

ABSTRACT

While continuous rotary calcination is a widely used thermal treatment in large-scale catalyst manufacturing, the process's heat and mass transfer mechanisms remain a challenge to characterize and to predict. Thus, the goal of this research is to improve fundamental understanding of rotary calcination to aid in the creation of a scientific methodology for process design and scale-up. For successful calcination to occur, the residence time of the particles must exceed the time required for heating and calcination at a set temperature. The optimal residence time therefore depends on both of these competing time scales, each of which is function of feed material properties, kiln geometry and kiln operating conditions. For uniform treatment of the feed, the particles must also exhibit low axial dispersion. In this work, the residence time distribution and axial dispersion coefficient for a dry cohesive fluid cracking catalyst powder were measured in a pilot plant kiln using a tracer study developed by Danckwerts. Results were successfully matched to the Taylor fit of the axial dispersion model and the Sullivan prediction for mean residence time. It was found that an increase in feed rate, kiln incline and rotary speed decreased mean residence time and overall axial dispersion. Such results have been established previously for free-flowing material like millimeter-sized extrudates, but have not been previously reported for the cohesive powders such as the one used in our work. As in free-flowing material, the axial dispersion coefficient was found to vary with kiln conditions. The values of the axial dispersion coefficients were lower for the powder than for free-flowing material, showing a dependency of axial dispersion on material properties as well as bulk flow behavior.

1. Introduction

With applications in a wide range of solids manufacturing processes including blending, drying, and calcining, the rotary kiln has established itself as an essential device in chemical and metallurgical industries (Brook et al., 1991). The device's popularity stems from its apparently simple geometry – the kiln operates by allowing gravity and rotation to move granular material or powder from one end to the other while the particles are heated. This mechanism has improved product quality in both batch and continuous processes (Brook et al., 1991), and researchers have performed analyses of the process as early as the 1920's (Sullivan et al., 1927). Still, the mass and heat transfer mechanisms in rotary kilns remain a challenge to characterize and to predict; developing fundamental understanding of rotary kiln processes will therefore greatly improve their scale-up from laboratory and pilot plant scales to manufacturing scale.

In preparation of chemical catalysts in particular, a better scientific understanding of rotary kilns will improve continuous calcination processes in which the particle bed exchanges heat with a freeboard gas and the kiln wall as it rotates and moves axially along the kiln (Fig. 1).

Successful calcination occurs when the particle residence time exceeds the time required for calcination. The typically long residence time of the material within the kiln favors uniform treatment of particles (Boateng, 2015), but long residence times lead to large material and energy costs. The key to successful and efficient calcination is then to minimize both the residence time and axial dispersion of particles within the kiln and to understand their relationship to the time required for calcination at a set temperature.

Radial and axial mixing are key factors that influence both

* Corresponding author.
E-mail address: cuitino@jove.rutgers.edu (A.M. Cuitiño).

http://dx.doi.org/10.1016/j.ces.2016.09.028
Received 19 May 2016; Received in revised form 18 September 2016; Accepted 24 September 2016
Available online 25 September 2016

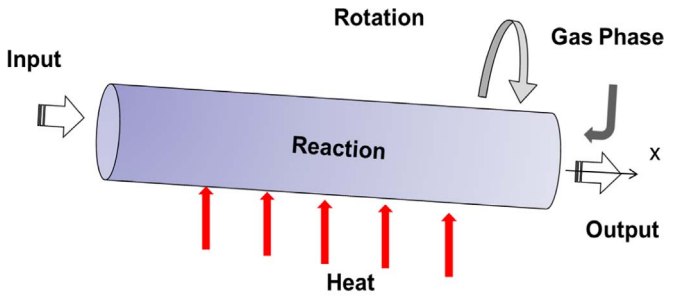

Fig. 1. Schematic of rotary kiln.

residence time and calcination time, and modifications such as lifters (also known as flights or baffles) have been installed in industrial kilns to improve mixing processes by increasing the surface area available for heat transfer (Mujumdar, 2014). The hot gas stream treats the material cascading from the lifters. This mechanism improves heat transfer by increasing the contact time between the gas and the material (Mujumdar, 2014). The hot particles remix with the cooler particle bed, improving heat transfer among the particles and effectively decreasing the time required to treat the material (Mujumdar, 2014; Saeman and Mitchell, 1954). The cascading rate of the lifters and kiln hold up, which is the total amount of materials in the kiln, determine the amount of material exposed to the hot gas flow (Saeman and Mitchell, 1954; Hirosue, 1989; Matchett and Baker, 1987). Several models and experimental studies have been published examining the effect of these lifter designs on heat and mass transfer (Hirosue, 1989; Matchett and Baker, 1987; Sheehan et al., 2005; Sunkara et al., 2013; Lee and Choi, 2013; Njeng et al., 2015a, 2015b, 2016; Sherritt et al., 1993, 1994; Chaudhuri et al., 2006). Many different lifter configurations like rectangular lifters, angular lifters, and circular lifters have been found in industry due to the range of applications employing rotary kilns (Mujumdar, 2014). Numerical simulations conducted by Chaudhuri et al. (2006) found L-shaped lifters to be more effective than rectangular lifters, though both enhance the rate of heat transfer and uniformity of the temperature profile for granular material within the kiln. The uniformity of the bed was found to be directly proportional to the number of lifters used (Chaudhuri et al., 2006). In a recent experimental study for mass transfer, Njeng et al. (2015a, 2015b, 2016) found that the use of lifters slightly increased the mean residence time of the particles. Njeng et al. (2015a) provided a prediction of the axial dispersion coefficient for lifted kilns based off their findings. It was found that the effect of the lifters on the axial dispersion coefficient became more pronounced with an increase in rotation rate and therefore material cascading rate, and slightly higher with increase in incline or smaller flow rate. Lifters also increased the mean residence time of the particles by forcing backflow of the material and minimized the effect of segregation on particle mixing by continuously remixing the particle bed (Njeng et al., 2015b, 2016).

Along with lifter configuration, a material's rheological properties, and the kiln's fill level, kiln incline, and rotation rate influence mixing by determining the mode of motion of the particles within the kiln. Six modes of motion – centrifuging, cataracting, cascading, rolling, slumping, and slipping – are possible (Sullivan et al., 1927). For the rolling mode, Saeman (1951) developed a model to compute the mean residence time based on material properties and kiln geometry. A predictive model for transverse mixing has also been developed by Sai et al. (1990) for particles in rolling mode. In general, these models assume that two layers, the passive and active layers, exist within the particle bed. The passive layer rotates with the kiln wall, and then rolls down the surface of the particle bed in a thin active layer. The time required for the particles to roll down the active layer is very small compared to the time spent in the passive layer.

Based on these studies, the speed of rotation, incline, and feed rate are found to affect the residence time and bed depth significantly. Gao et al. (2013) found that feed rate has little impact on the mean residence time, though Njeng et al. (2015a, 2015b, 2016) found that an increase in mass flow rate showed a decrease in the mean residence time. Studies have also shown that the mean residence time scales with particle aspect ratio and is inversely related to rotary speed and kiln incline (Njeng et al., 2015a, 2015b, 2016; Sherritt et al., 1993, 1994; Gao et al., 2013). While recognizing such trends aid in kiln operation, the mean residence time alone cannot provide insight into the axial dispersion of the particles. For this, the residence time distribution, a probability distribution characterizing the flow profile of a material, must be measured (Sai et al., 1990; Gao et al., 2012, 2011). The width of the distribution depends on material flow determined by inherent properties and operating conditions. Narrower distributions are indicative of yielding a more uniform product and therefore overall less axial dispersion. Previous studies have shown that narrower residence time distributions correspond to high feed rate, high incline, and fast rotation rates (Njeng et al., 2015a, 2015b, 2016; Sherritt et al., 1993, 1994; Gao et al., 2013). The axial dispersion coefficient can be measured experimentally by injecting tracer particles and observing these particles at the outlet using a methodology developed by Danckwerts (1953) to obtain the residence time distribution. Prior experiments have shown that axial dispersion coefficient increases with rotation rate and decrease with an increase in feed rate and kiln incline. In performing a tracer study in a pilot plant kiln operated at room temperature, Gao et al. (2013) found that the axial dispersion coefficient of millimeter-sized particles decreased with rotary speed and incline angle. Higher feed rates and larger angle of repose of the materials led to higher fill levels, reducing axial dispersion. Njeng et al. (2015a, 2015b, 2016) found similar trends in broken rice and sand. These studies were conducted on relatively large particles where the effect of cohesion is negligible (Njeng et al., 2015a, 2015b, 2016; Gao et al., 2013).

For cohesive particles, some studies have reported conflicting results regarding the effect of cohesion on the axial dispersion (Rietema, 1984; Sherritt et al., 2003; Sudah et al., 2002; Gupta et al., 1991; Alexander et al., 2002; Rao et al., 1991; Shinbrot et al., 1999). Experiments by Rutgers, (1965) have shown that cohesive material leads to a higher axial dispersion coefficient, while some simulations and experiments by Sudah et al. (2002) and Gupta et al. (1991) have shown that low degree of cohesion increases mixing, while high cohesion slows mixing. Koynov et al. (2016) measured the axial dispersion coefficient for cohesive powders using Fick's second law in a batch system with and without lifters. Koynov et al. (2016) found that changes in fill level and the presence of baffles did not significantly change the value of the axial dispersion coefficient, but their experimental step up did not allow for correlating the effect of bulk flow with the axial dispersion coefficient.

The aim of the present study is to investigate the effects of operating conditions on the mean residence time and axial dispersion coefficient of dry cohesive powders in rotatory kiln with lifters. The effects of feed rate, kiln incline, and kiln rotation rate on residence time and particle distribution were studied.

2. Materials and methods

2.1. Materials

Zeolitic fluidized cracking catalyst (FCC) powder (W.R. Grace Davison, Columbia, Maryland, USA) was selected as the feed material. This powder was chosen because of its indusrun relevance and to further extend the library of materials used in previous work. Fig. 2 shows the particle size distribution of the FCC powder. The d10, d50, and d90 of the powder are 46, 80, and 140, respectively. Since lifters diminished the effect of segregation by continuously remixing the powder (Njeng et al., 2016), the effects of segregation due to particle

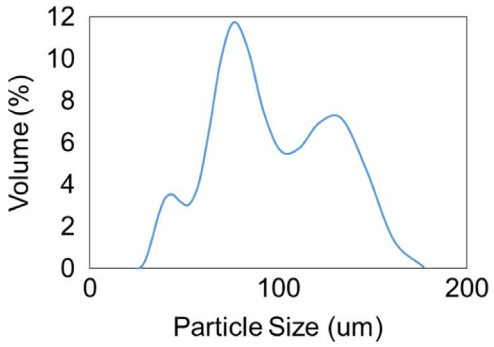

Fig. 2. Particle size distribution for FCC Powder.

size were neglected. The loose bulk density was measured using the mass of material required to fill a 100 mL graduated cylinder. The powder has a bulk density of 0.76 g/cm^3. The static angle of repose was as measured using a fixed funnel. The material was poured through a funnel to form a cone of a predetermined width of 2 in. The height of the cone was then measured and used to calculate the static angle of repose, which was found to be 37.0°.

Dyed tracer particles were made via incipient wetness impregnation of the FCC powder with cobalt (II) nitrate hexahydrate. The powder contained 10 wt% cobalt oxide following calcination at 538 °C for 8 h. The measured loose bulk density and the static angle of repose of the material were unchanged by the dying process.

2.2. Experimental setup

Experiments were conducted in a pilot plant rotary kiln at atmospheric temperature and pressure. The kiln had an internal diameter of 4 in. and a length of 90 in., giving an L/D ratio of 22.5. Three sets of lifters spanned 70% of the kiln length, starting from the inlet. Each set contained four lifters, five inches apart from each other set equiangular from each other along the circumference of the kiln. Each lifter had a base of 2.5 in., a height of 0.25 in. and a length of 8.5 in. (Fig. 3a).

The matrix of experiments conducted is summarized in Table 1. Operating conditions were chosen based on previous experiments (Gao et al., 2013) and equipment capabilities. A screw feeder fed material into the kiln at constant rates of 11.2 cm^3/min or 48.9 cm^3/min. A control panel set kiln speeds to 3.5, 4.0 or 4.5 rpm. A jack mechanism at the inlet of the kiln adjusted the incline angle to 2.0° or 4.0°. A fixed circular dam at the inlet prevented backward leakage of materials; the maximum operating fill level without backward leakage was about 15%. Operating fill levels during experiments were calculated to range from 2% to 10%.

2.3. Methods

A pulse test method developed by Danckwerts (1953) was used to determine the residence time distribution. Undyed powder was fed into the kiln at a constant feed rate. At steady state, the kiln was turned off for approximately one minute to inject 7 g of tracer particles into the kiln using a spoon 2.5 in. long, 2 in. wide and 1.5 in. deep. The tracer was injected from the top of the bed 45 in. from the kiln outlet to allow ample time for mixing and to minimize end effects (Fig. 3b). Since the kiln was off for an average of 3% of the mean residence time, a pulse injection was assumed, and the spoon dimensions were neglected in analysis of the data. At the kiln outlet, mixtures of the undyed material and tracer were then manually collected in 30 s intervals using a sample cup held directly below the center of the face of the outlet. Samples were collected until black tracer powder was no longer visible to the eye.

The tracer concentration in each sample was determined using a spectrophotometer (ColorFlex EZ, HunterLab) following a methodology developed by Emady et al. (2015). Prior to the performance of tracer studies, mixtures of tracer and undyed powder were created, each containing a different ratio of tracer particles to undyed powder. Concentrations above 20% were not observed after samples from experiments were read, thus mixtures of 0%, 5%, 10%, 15%, and 20% were used in the final calibration. To ensure the tracer and undyed material were well-mixed, each sample calibration mixture was placed on a rotating rack for at least one hour. A sample of each calibration mixture was transferred to the sample port of the spectrophotometer and flashed with a beam of light to obtain its % reflectance. The ideal sample size was determined by comparing the variability between 1 g samples and 5 g samples, the maximum capacity of the spectrophotometer sample port. The variability was determined by measuring the standard deviation across the readings. It was found that the readings of 5 g samples produced less variability due to reduced movement of particles within the sample port. Still, variability existed, with a standard deviation between readings of 0.67, so an average of 5 readings per mixture was taken as the characteristic % reflectance of the mixture. Between each reading, the samples were mixed in the original vial containing the mixture by rotating the vials, this time for at least one minute. The spectrophotometer provided readings from wavelengths of 400–700 nm in increments of ten nanometers.

In Fig. 4a, the five % reflectance vs. wavelength curves and their average obtained for a mixture containing 15 wt% tracer particles are presented as an example of the data obtained from the spectrophotometer. The manufacturer's guidelines for use of the device stated that rotation of the circular sample cup within the port in 90° intervals between each reading would ensure that light hit the sample from all possible angles. Five readings were therefore taken at 0°, 90°, 180°,270° and 360°. The signal received by spectrophotometer by the mixtures from wavelengths of 540–650 nm nanometers was almost constant, indicating a steady signal from the spectrophotometer within this range of wavelengths. This range was therefore used to generate calibration curves relating the % reflectance of each mixture to its concentration of tracer. The wavelength of 560 nm was selected for the concentration curve as it produced the smallest error among curves

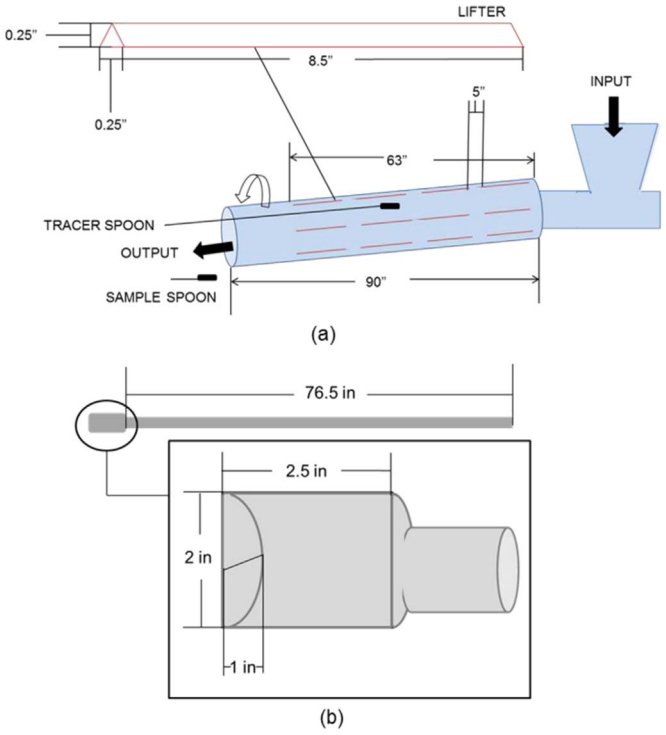

Fig. 3. (a) Schematic of rotary kiln and lifters. (b) Diagram of spoon used for tracer injection.

Table 1
Experimental matrix of kiln operating conditions.

Operating variables	Conditions
Incline angle (deg)	2.0, 4.0
Rotary speed (rpm)	3.5, 4.0, 4.5
Volumetric feed rate (cm^3/min)	11.2, 48.9

generated using wavelengths from 540 to 650 nm. The 560 nm wavelength was selected because the standard deviation from the five readings (Fig. 4a) was the lowest at this wavelength. The calibration curve, a linear fit, is shown in Fig. 4b, where y represents the % reflectance (%) at 560 nm and x represents the concentration $C(t)$ of the mixture (wt%). The curve showed that as the amount of tracer increased, the lower the % reflectance. This was expected as the darker samples contained more tracer particles.

The calibration curve provided with a concentration curve for the tracer at each operating condition. An example of the concentration curves obtained from the raw % reflectance versus concentration data is shown Fig. 5a, which shows a comparison of concentration profiles for five runs from the same experimental setup. The kiln was emptied at the end of each run to measure holdup, then refilled for operation until steady-state conditions were reached for the next run. Though the profiles for each run are not exactly the same, the small differences are consistent within experimental error. As seen in Fig. 5a, the relationship sometimes predicts that the sample has a negative concentration due to errors associated with calibration. At these time points, concentration of the tracer is assumed to be 0%. To account for this, the curve produced for each run was adjusted by adding the smallest concentration predicted to each concentration, setting all negative values to zero. The adjusted curve can be found in Fig. 5b. Then, the average concentration curve for a given setup was computed based on the adjusted concentration curve. The average concentration was used for analysis of the residence time distribution and axial dispersion of the particles.

The residence time distribution was then calculated by using the following equation (Gao et al., 2013; Gao et al., 2012):

$$E(t)=\frac{C(t)}{\int C(t)dt} \tag{1}$$

where $E(t)$ is the residence time distribution and $C(t)$ is the concentration of tracer particles at time t.

The axial dispersion model was used to represent the residence time distribution under the following assumptions (Gao et al., 2012):

(i) the conditions reached steady state;

(ii) a delta-dirac tracer pulse was a function only of time and axial position;

(iii) the axial convective velocity and axial dispersion coefficient of tracer particles was constant for stable operating conditions.

The model considers axial motion of the particles as two components: a convective component arising from the bulk motion of the material and a diffusive component arising from the random motion of the particles. Cohesive forces are not considered, and so this method, previously used for free-flowing materials, was tested in our experiments. This can be represented by the Fokker-Planck equation, which describes the evolution of particle distribution in continuous systems (Gao et al., 2012):

$$\frac{\partial C}{\partial t}=\frac{1}{Pe}\frac{\partial^2 C}{\partial x^2}-\frac{\partial C}{\partial x} \tag{2}$$

Where

$$Pe=\frac{l}{V_x D_{ax}} \tag{3}$$

where Pe is the Peclet number, l is the length traveled by the tracer, D_{ax} is the axial dispersion coefficient, and v_x is the axial velocity of the particles. The Taylor (Gao et al., 2012) dispersion solution is presented:

$$E(\varepsilon,\ \theta)=\frac{Pe^{0.5}}{(4\pi\theta)^{0.5}}e^{-\frac{Pe(\varepsilon-\theta)^2}{4\theta}} \tag{4}$$

Where $\theta=\frac{t}{\tau}$ and $\varepsilon=\frac{x}{l}$ represent the dimensionless time and location of the material in the kiln, respectively; and τ is the mean residence time, implicitly calculated from the experimental data.

The mean residence time was also determined experimentally from the mass holdup, measured at the end of each experiment by shutting off the feed and collecting the powder remaining in the kiln:

$$\tau_{holdup}=\frac{M}{\dot{m}} \tag{5}$$

Where τ_{holdup} is the mean residence time, M is the mass hold up, and $\dot{m}$ is the mass flow rate of the material.

The measured τ_{holdup} was then used to validate the prediction of mean residence time proposed by Sullivan:

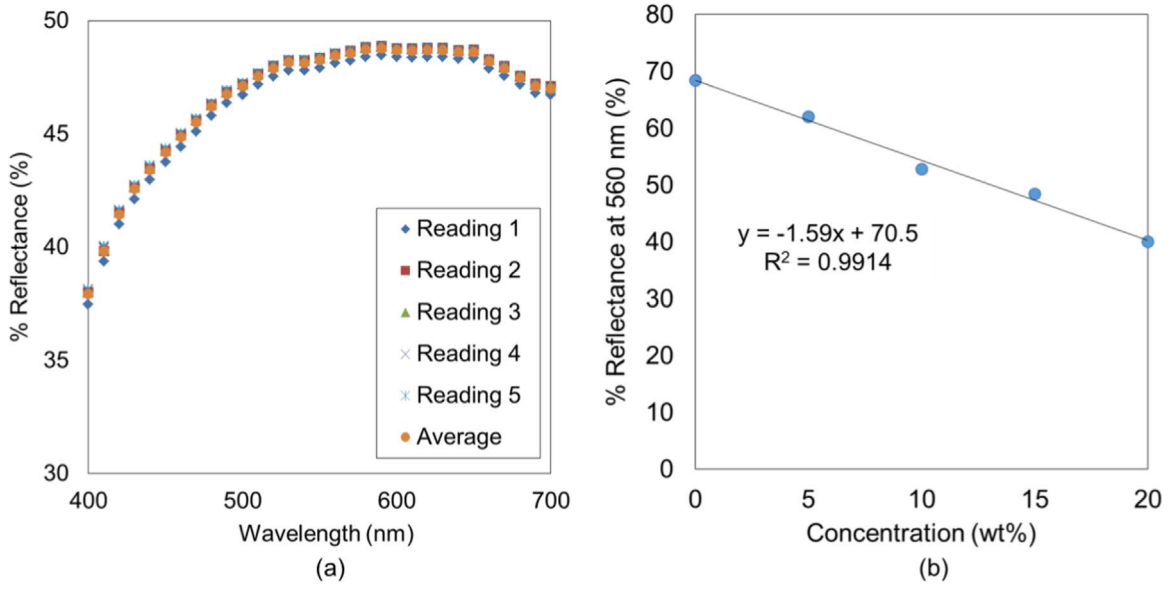

Fig. 4. (a) % An example of % reflectance (%) vs. wavelength (nm) data obtained from spectrophotometer from wavelengths of 540–650 nm for a sample containing 15 wt% tracer. (b) The data from at 560 nm was used to used to fit a curve relating % reflectance (%) to tracer concentration (wt%).

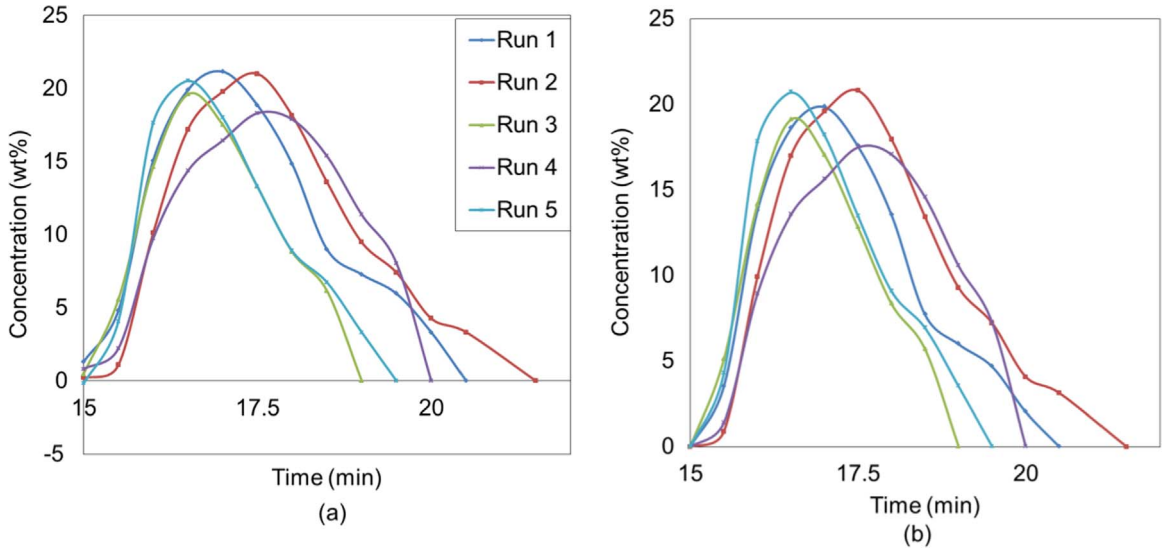

Fig. 5. (a) An example of the raw concentration vs. time curve obtained from the calibration curve for each run at a calciner incline of 2.0°, feed rate of 11.2 cm^3/min and a rotation rate of 3.5 rpm. (b) The concentration curve was adjusted to obtain positive values for concentration.

$$\tau_{Sullivan}=\frac{1.77(\theta)^{0.5}Lf}{\varphi DN} \quad (6)$$

Where θ is the angle of repose of the material, L is the length of the kiln, φ is the incline of the kiln, D is the diameter of the kiln, and N is the rotary speed. A factor for flow f is to account for obstructions in flow due to modifications such as lifters. A value of f=1 was initially assumed for this system despite the presence of lifters to observe the magnitude of their impact on the predicted mean residence time. Following experiments, the value of f was then calculated as the ratio of τ_{holdup} to $\tau_{Sullivan}$ to measure the experimental deviation from the predicted residence time:

$$f=\frac{\tau_{holdup}}{\tau_{Sullivan}} \quad (7)$$

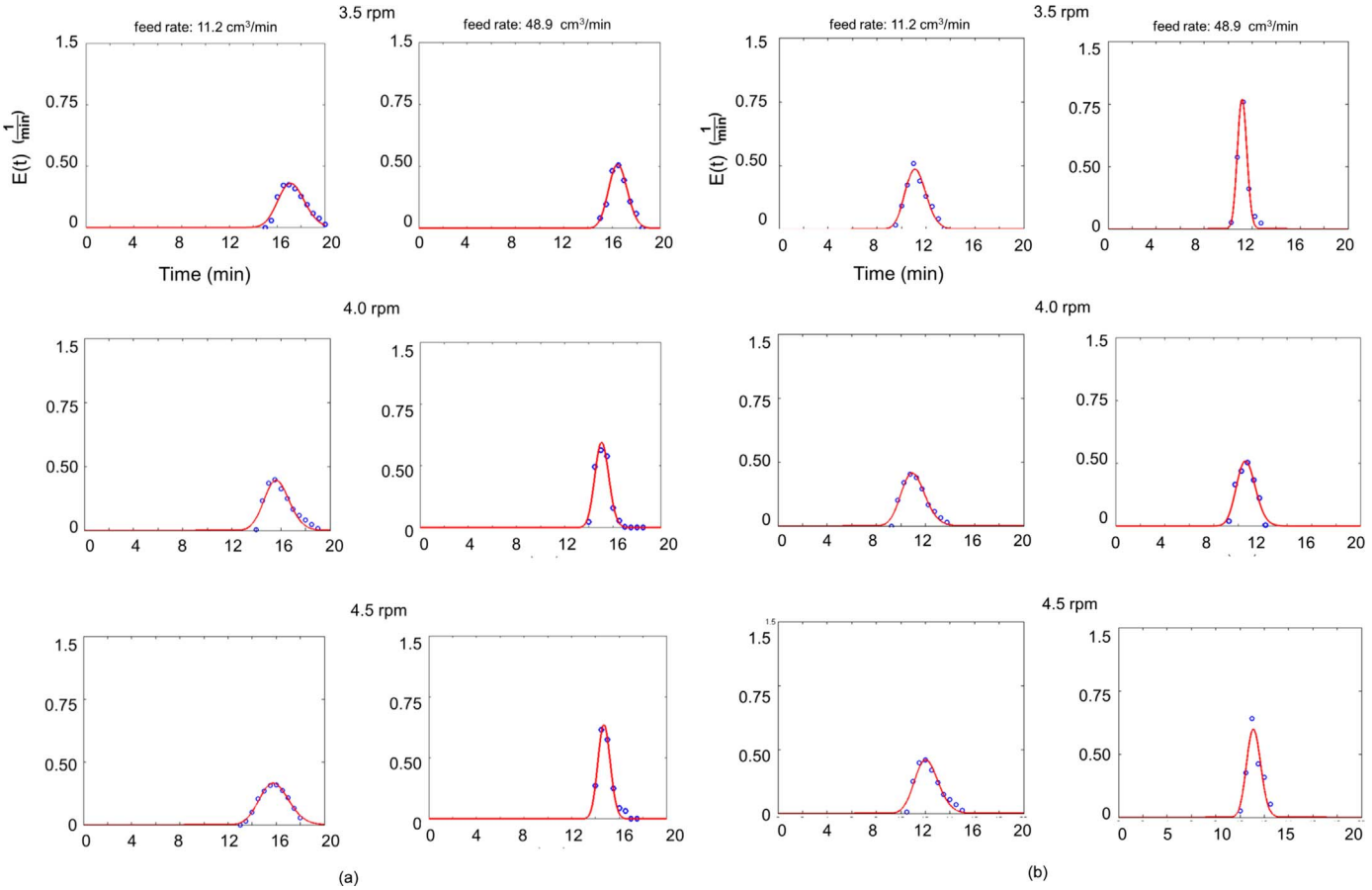

Fig. 6. Residence time distributions obtained at (a) 2° and (b) 4°. Each column indicates the feed rate at which the residence time distribution was obtained. Each row indicates the rotary speed at which the rotary speed was obtained.

3. Results and discussion

3.1. Residence time distribution and axial dispersion coefficient

Good agreement with the Taylor Dispersion model was found (Fig. 6). Each row displays residence time distributions obtained at a different rotary speed. As rotary speed increased, the residence time distribution slightly shifted to shorter times due to the increased velocity of the particles. The overall mean residence time, depicted by the peak of the distribution, slightly decreased. This was due to an increase in the axial velocity of the particles with rotary speed. As rotary speed increased, particles exchanged between the passive and active layers at a faster rate. The more particles that moved into the active layer, more particles moved down the kiln length, reducing their time spent in the kiln. Comparing Fig. 6a to b, it was found that this effect was enhanced by an increase in the incline angle of the kiln, which encouraged the particles to slide down the kiln length as they exchanged between the passive and active layers.

An increase in incline also narrowed the residence time distribution at 3.5 rpm, but not for 4.0 and 4.5 rpm. This indicated that at 3.5 rpm, particles spent less time mixing within the kiln and more time traveling towards the outlet. This may be due to low lifter action at this rotation rate. An increase incline decreased the fill level of the kiln, and thus the ratio of the particle bed height to lifter height. Keeping feed rate constant, the ratio of the amount of powder lifted by the lifters to the particle bed therefore increased. Increasing the rotation rate from 3.5 to 4.5 rpm, the cascading rate of the lifters also increased, so that the amount of material experiencing backflow increased. This may have hindered the narrowing of the distribution at 4.0 and 4.5 rpm.

Comparing each column in (a) and again in (b), it was found that an increase in feed rate also narrowed the residence time distribution. At the higher feed rate, the fine FCC powder displayed behavior closer to the “plug flow” model applied to the kiln, in which the particles of the feed all exit the kiln at the same time. This “plug flow” behavior contributed heavily to the axial velocity of the particles, charging their passage through the kiln. Hence, overall dispersion decreased since mixing time decreased. This effect even limited the effect of rotary speed on the mean residence time – an increase of feed rate had no influence on the mean residence time. Rather than couple the effect of rotary speed on the mean residence time, the feed rate instead dominated the contribution of the rotary speed on the axial velocity.

Narrow residence time distribution corresponded to relatively low axial dispersion coefficients at each incline (Fig. 7). The highest axial dispersion coefficients were obtained with the lower feed rate and higher incline angle at all rotation speeds. This was unexpected. At high incline, the particle bed's velocity is greater, and so the mean residence time decreases. However, an increase incline decreases the fill level of the kiln, and thus the ratio of the particle bed height to lifter height. From 3.5 to 4.5 rpm, the cascading rate of the lifters increases, so that the amount of material experiencing backflow increases, providing an explanation for the increase in the axial dispersion coefficient from 3.5 to 4.0 rpm at a 4° incline for both feed rates. At the low feed rate, however, the fraction of lifted material is greater, so that dispersion is overall greater. The decrease in the axial dispersion coefficient from 4.0 to 4.5 rpm may be due to the fact the particle's axial velocity is at its maximum, pushed by rotation and the incline. This push may make the particles move too quickly past the lifters to allow for sufficient mixing, decreasing the axial dispersion coefficient.

When compared to the axial dispersion coefficients obtained from free-flowing material in experiments conducted by Gao et al. (2013), the range of values obtained for FCC powder were closest in value to those obtained for the cylindrical and quadrilobe extrudates. These high-aspect ratio particles flowed much less smoothly than the spheres; they exhibited relatively high friction which hindered their free flow, leading to axial dispersion coefficients that close to those for a cohesive material like FCC powder. Still, the overall values for D_{ax} were lower for the powder, indicating a dependency on material properties. The effect of bulk flow, however, was still found significant; the values of the axial dispersion coefficient also exceeded the value predicted for the same material by Koynov et al. (2016). In their study, D_{ax} was calculated using Fick's second law and therefore neglected the impact of bulk flow. Their values ranged from 0.95 to 0.99 cm^2/min, while in our work, values ranged from 0.77 cm^2/min to 4.7 cm^2/min (Fig. 7). Our results therefore showed that the influence of bulk flow was significant on the axial dispersion coefficient.

3.2. Mean residence time

The observations from the Taylor model were consistent with the mean residence time measurements based on the total mass hold up and the prediction from the Sullivan model. For our experiments, the mean residence time ranged between 9 and 19 min. The mean residence time decreased as the speed of rotation and angle of incline increased (Fig. 8). The Taylor model and the mass hold up τ show that feed rate has little impact on the mean residence time. The predictions from Sullivan model were generally an underestimation of the experimental residence time. An underestimation of the residence time was consistent with the results of Njeng et al. (2015a, 2015b), who found that lifters, regardless of shape, increased the residence time of solids. A more thorough understanding of the mechanism requires study of the discharge rate of the lifters.

At low incline, the experimental τ was 1.7–2.9 min above the Sullivan prediction for low feed conditions, and 0.3–5.4 min above the Sullivan prediction for high feed. At high incline, the experimental τ was 4.6–6.7 min above the Sullivan prediction for low feed, and 2–8 min above the Sullivan prediction for high feed. This was expected, since the Sullivan model assumes unobstructed flow. The deviations of the Sullivan model from the experimental mean residence time were quantified using Eq. (7). Values of f were higher at 4° than at 2°, but varied little within each incline (Table 2). At 4° f approached values of 2, indicating that the predicted residence time was almost half of the measured mean residence time. Deviations may have increased because of increased lifter action due to the decrease in fill level at high incline. Experiments conducted at 4° for high feed at a rotation rate of 4.5 rpm were an exception; perhaps the low fill level of roughly 2% caused a change of motion in the particle bed. Perhaps at this rotation rate, the particle velocity increased to a point where lifter action was diminished, and the particles surpassed the lifters as they cascaded.

4. Conclusions

Predictive models for the mean residence time remain applicable to continuous calcination systems even in the presence of lifters. Residence time distribution theory stands even for the cohesive powder studied, and trends found in previous work were again observed. Feed

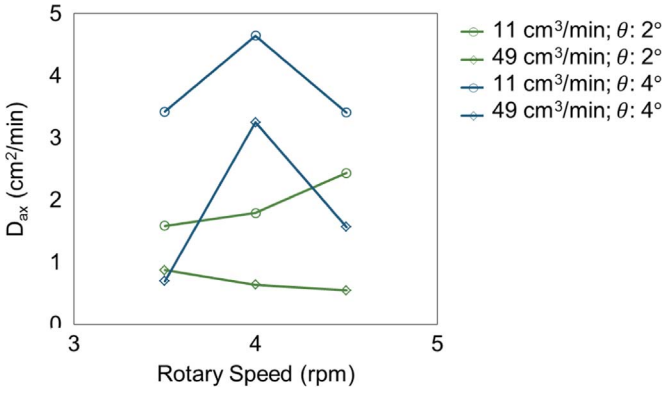

Fig. 7. Axial dispersion coefficient D_{ax} obtained from the Taylor fit.

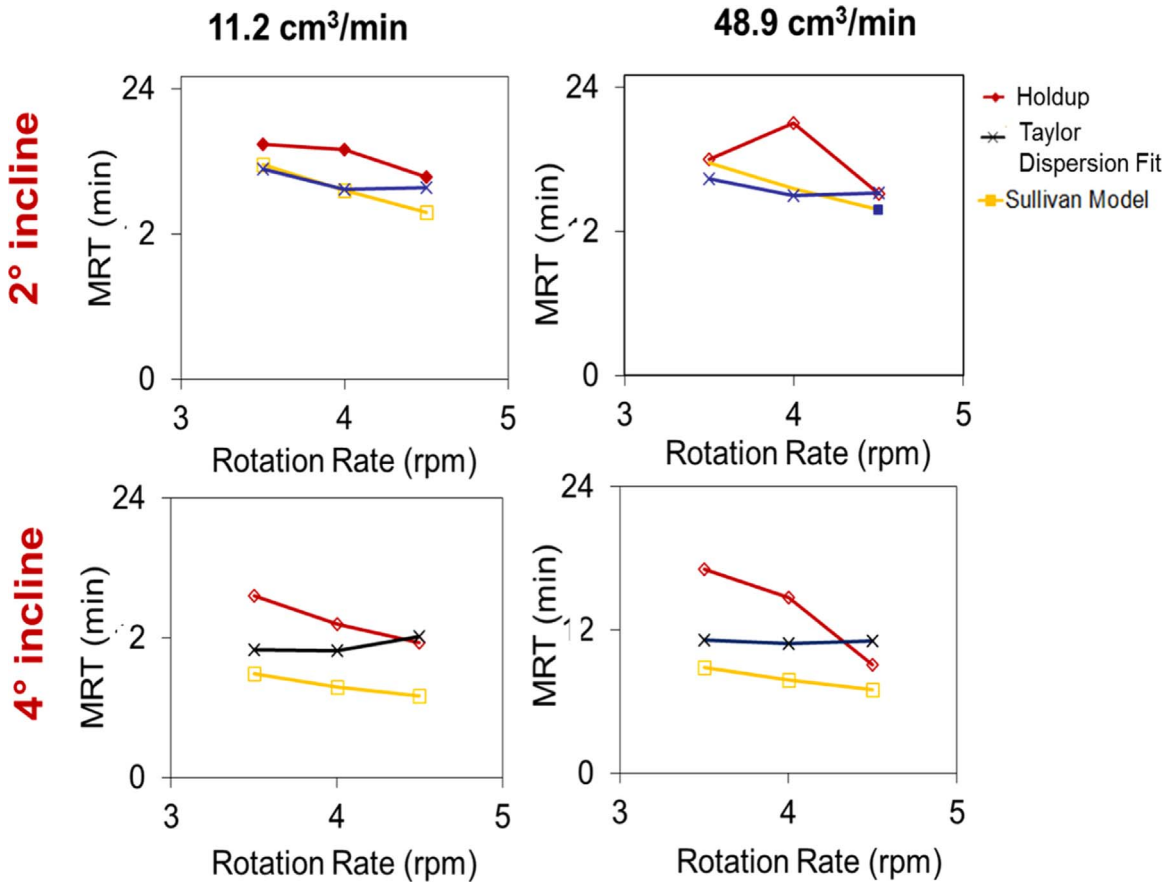

Fig. 8. Plots of the average mean residence time versus rotation rate at each operating condition. The mean residence times are determined experimentally from the holdup and Taylor dispersion fit and predicted by the Sullivan model.

Table 2
Calculated values of flow factor *f*.

		Incline (deg)	
		2	4
Feed rate (cm^3/min)	Rotary speed (rpm)	f	
11.2	3.5	1.1	1.8
	4	1.2	1.7
	4.5	1.2	1.7
48.9	3.5	1.0	1.9
	4	1.3	1.9
	4.5	1.1	1.3

rate had little effect on mean residence time, but narrowed residence time distribution; increases in rotation rate and kiln incline decreased mean residence time, and therefore shifted the residence time distribution to shorter time regions. Kiln incline affected mean residence time more than any other operating condition, reducing the predicted mean residence time by an average of 26%. Still, a small set of operating conditions was examined here – two feed rates, with the larger five times that of the smaller one, three rotation rates only with a range of 1 rpm, and two inclines with a range of two degrees. Intermediate feed rates and a broader range of rotation rates and inclines should be examined. While the presence of lifters had little effect on mean residence time, their effect on flow should be further investigated as well to better predict the deviation from predictive models. The effect of their presence on axial and radial mixing should also be further explored. Deeper understanding of the effect of cohesion on particle flow, particularly on axial dispersion, is also necessary. The material studied here behaved similarly to free-flowing material, but more experiments with other powders varied in cohesivity and size, should be examined.

Once mass transfer studies provide a better understanding of flow in rotary kilns experiments should also be done at high temperatures to observe the effect of heat on material flow. Understanding of such factors will aid in optimization of continuous rotary kiln processes.

Acknowledgements

This work was supported by the Rutgers Catalyst Manufacturing Science and Engineering Consortium. The authors would also like to acknowledge W.R. Grace Davison for providing the catalyst powder used in this study.

References

Alexander, A., Shinbrot, T., Muzzio, F.J., 2002. Scaling surface velocities in rotating cylinders as a function of vessel radius, rotation rate, and particle size. Powder Technol. 126 (2), 174–190.
Boateng, A.A., 2015. Rotary Kilns: Transport Phenomena and Transport Processes. Butterworth-Heinemann, Oxford, UK.
Brook, R., Cahn, R., Bever, M., 1991. Concise Encyclopedia of Advanced Ceramic Materials. Pergamon Press, Oxford.
Chaudhuri, B., Muzzio, F.J., Tomassone, M.S., 2006. Modeling of heat transfer in granular flow in rotating vessels. Chem. Eng. Sci. 61 (19), 6348–6360.
Danckwerts, P.V., 1953. Continuous flow systems: distribution of residence times. Chem. Eng. Sci. 2 (1), 1–13.
Emady, H.N., Wittman, M., Koynov, S., Borghard, W.G., Muzzio, F.J., Glasser, B.J., Cuitino, A.M., 2015. A simple color concentration measurement technique for powders. Powder Technol. 286, 392–400.
Gao, Y., Vanarase, A., Muzzio, F., Ierapetritou, M., 2011. Characterizing continuous powder mixing using residence time distribution. Chem. Eng. Sci. 66 (3), 417–425.
Gao, Y., Muzzio, F.J., Ierapetritou, M.G., 2012. A review of the residence time distribution (RTD) applications in solid unit operations. Powder Technol. 228, 416–423.

Gao, Y., Glasser, B.J., Ierapetritou, M.G., Cuitino, A., Muzzio, F.J., Beeckman, J.W., Fassbender, N.A., Borghard, W.G., 2013. Measurement of residence time distribution in a rotary calciner. AIChE J. 59, 4068–4076. http://dx.doi.org/10.1002/aic.14175.

Gupta, S.D., Khakhar, D.V., Bhatia, S.K., 1991. Axial segregation of particles in a horizontal rotating cylinder. Chem. Eng. Sci. 46 (5), 1513–1517.

Hirosue, H., 1989. Influence of particles falling from flights on volumetric heat transfer coefficient in rotary dryers and coolers. Powder Technol. 59 (2), 125–128.

Koynov, S., Wang, Y., Redere, A., Amin, P., Emady, H.N., Muzzio, F.J., Glasser, B.J., 2016. Measurement of the axial dispersion coefficient of powders in a rotating cylinder: dependence on bulk flow properties. Powder Technol. 292, 298–306.

Lee, H., Choi, S., 2013. Lifter design for enhanced heat transfer in a rotary kiln reactor. J. Mech. Sci. Technol. 27 (10), 3191–3197.

Matchett, A.J., Baker, C.G.J., 1987. Particle residence times in cascading rotary dryers. Part 1–derivation of the two-stream model. J. Sep. Process Technol. 8 (4), 11–17.

Mujumdar, A.S. (Ed.), 2014. Handbook of Industrial Drying. CRC Press, Boca Raton, FL.

Njeng, A.B., Vitu, S., Clausse, M., Dirion, J.L., Debacq, M., 2015a. Effect of lifter shape and operating parameters on the flow of materials in a pilot rotary kiln: Part I. Experimental RTD and axial dispersion study. Powder Technol. 269, 554–565.

Njeng, A.B., Vitu, S., Clausse, M., Dirion, J.L., Debacq, M., 2015b. Effect of lifter shape and operating parameters on the flow of materials in a pilot rotary kiln: Part II. Experimental hold-up and mean residence time modeling. Powder Technol. 269, 566–576.

Njeng, A.B., Vitu, S., Clausse, M., Dirion, J.L., Debacq, M., 2016. Effect of lifter shape and operating parameters on the flow of materials in a pilot rotary kiln: Part III. Up-scaling considerations and segregation analysis. Powder Technol. 297, 415–428.

Rao, S.J., Bhatia, S.K., Khakhar, D.V., 1991. Axial transport of granular solids in rotating cylinders. Part 2: experiments in a non-flow system. Powder Technol. 67 (2), 153–162.

Rietema, K., 1984. Powders, what are they? Powder Technol. 37 (1), 5–23.

Rutgers, R., 1965. Longitudinal mixing of granular material flowing through a rotating cylinder: part II. Experimental. Chem. Eng. Sci. 20 (12), 1089–1100.

Saeman, W.C., 1951. Passage of solids through rotary kilns. Chem. Eng. Process. 47, 508–514.

Saeman, W.C., Mitchell, T.R., 1954. Analysis of rotary dryer and cooler performance. Chem. Eng. Prog. 50 (9), 467–475.

Sai, P.S.T., Surender, G.D., Damodaran, A.D., Suresh, V., Philip, Z.G., Sankaran, K., 1990. Residence time distribution and material flow studies in a rotary kiln. Metall. Trans. B 21 (6), 1005–1011.

Sheehan, M.E., Britton, P.F., Schneider, P.A., 2005. A model for solids transport in flighted rotary dryers based on physical considerations. Chem. Eng. Sci. 60 (15), 4171–4182.

Sherritt, R.G., Caple, R., Behie, L.A., Mehrotra, A.K., 1993. The movement of solids through flighted rotating drums. Part 1: model formulation. Can. J. Chem. Eng. 71, 337–346.

Sherritt, R.G., Caple, R., Behie, L.A., Mehrotra, A.K., 1994. The movement of solids through flighted rotating drums. Part 2: solids gas interactions and model validation. Can. J. Chem. Eng. 72 (2), 240–248.

Sherritt, R.G., Chaouki, J., Mehrotra, A.K., Behie, L.A., 2003. Axial dispersion in the three-dimensional mixing of particles in a rotating drum reactor. Chem. Eng. Sci. 58 (2), 401–415.

Shinbrot, T., Alexander, A., Muzzio, F.J., 1999. Spontaneous chaotic granular mixing. Nature 397 (6721), 675–678.

Sudah, O.S., Coffin-Beach, D., Muzzio, F.J., 2002. Effects of blender rotational speed and discharge on the homogeneity of cohesive and free-flowing mixtures. Int. J. Pharm. 247 (1), 57–68.

Sullivan, J.D., Maier, C.G., Ralson, O.C., 1927. Passage of Solid Particles Through Rotary Cylindrical Kilns. Bureau of Mines Technical Paper, US.

Sunkara, K.R., Herz, F., Specht, E., Mellmann, J., 2013. Influence of flight design on the particle distribution of a flighted rotating drum. Chem. Eng. Sci. 90, 101–109.